Isospin-density-dependent pairing from infinite nuclear matter to finite nuclei

Xu Meng, Shisheng Zhang ⬝,* and Lin Guo ⬝
School of Physics, Beihang University, Beijing 100191, China

Lisheng Geng†
School of Physics, Beihang University, Beijing 100191, China;
Beijing Key Laboratory of Advanced Nuclear Materials and Physics, Beihang University, Beijing 100191, China;
School of Medicine and Engineering, Beihang University, Beijing, 100191, China;
and School of Physics and Microelectronics, Zhengzhou University, Zhengzhou, Henan 450001, China

Ligang Cao ⬝‡
College of Science and Technology, Beijing Normal University, Beijing 100875, China

The effective isospin-density-dependent pairing interaction (P1) [S. S. Zhang, U. Lombardo, and E. G. Zhao, Sci. Chin. Phys. Mech. Astron. **54**, 236 (2011)] extracted from neutron pairing gaps for $^1S_0$ in asymmetric nuclear matter calculations [S. S. Zhang, L. G. Cao, U. Lombardo, E. G. Zhao, and S. G. Zhou, Phys. Rev. C **81**, 044313 (2010)] is employed to study the bulk properties of Ca, Ni, Zr, and Sn isotopes. The odd-even mass (OEM) staggering is calculated by the Skyrme Hartree-Fock plus BCS method (SHF+BCS) with the SkP force. For comparison, we study two other types of isovector effective pairing interactions. One is also extracted from pairing gaps of infinite nuclear matter by the Brueckner-Hartree-Fock (BHF) method but for free spectrum (P2). The other is obtained by fitting the empirical OEM (P3). An isoscalar effective pairing interaction (P4) is also adopted, which is determined by fitting the empirical OEM. We find that interaction P1 can better describe the OEM staggering of Ni, Zr, and Sn isotopes by 14.3%, 41%, and 30.4% compared with interaction P2, in terms of root-mean-square deviations to the empirical OEM, respectively. On the other hand, the performance of P1 and P2 is comparable for Ca isotopes. For Ca and Ni isotopes, P1 behaves similarly to P3, but for Zr isotopes P1 is better than P3 by ≈34%. One may conclude that the isovector pairings are preferred over the isoscalar one for neutron pairings in finite nuclei with the SkP force. It is quite interesting to note that the pairing interaction P1 extracted from nuclear matter calculations can describe pairing gaps of finite nuclei as well as or even better than the interaction P3 directly fitted to finite nuclei. To study the influence from the mean fields on the OEM, we perform the same analysis using the SLy4 and SkI4 forces as well. It turns out that pairing gaps described by these two forces with four pairing interactions are underestimated, so that P2 seems to be better than P1 and is comparable with P3.

I. INTRODUCTION

Pairing correlations play an important role in describing many observables and processes in nuclear physics, for instance, the odd-even mass (OEM) staggering for finite nuclei [1,2], the superfluidity and cooling of neutron stars [3,4], *r*-process nucleosynthesis [5], etc.

Tremendous efforts have been made to extract pairing interactions from different observables. One way is to fit the OEM staggering of finite nuclei via the empirical three-point or five-point pairing gap formulas with the experimental binding energies as inputs [6,7]. But pairing gaps can be different for three-point and five-point formulas, and sometimes can-

not reproduce small pairing for nuclei with (double) magic numbers or truly reflect the experimental OEM difference since energy density functionals for odd-*A* systems are not as good as those for even-even systems [8]. Recently, there is a proposal that nucleonic pairing can be extracted from nuclear density functional theory for pairing rotational bands in even-even nuclei with the quasi-particle random-phase approximation (QRPA) method [8]. A separable force of finite range is widely used to describe pairing correlations in normal nuclei [9] and has recently been applied to provide effective pairing interactions for hyperons [10]. Another alternative is to extract pairing interactions from asymmetric nuclear matter (ANM) calculations with the microscopic Brueckner-Hartree-Fock (BHF) method [1,2,11–15] and adopt the local density approximation to obtain the isospin-density-dependent parameters for finite nuclei. In the last decade, Margueron, Sagawa, and Hagino introduced zero-range isospin-density-dependent effective pairing interactions [11,16] by fitting to

---
*zss76@buaa.edu.cn
†lisheng.geng@buaa.edu.cn
‡caolg@bnu.edu.cn

the corresponding pairing gaps of symmetric nuclear matter (SNM) and pure neutron matter (PNM) obtained by the BHF method with and without medium polarization effect [17]. But those pairing gaps presented in Ref. [16] are extracted from free spectrum instead of the mean field spectrum, as clarified in our previous paper [1]. In that paper, we proposed a new effective pairing interaction [1] from the mean field spectrum based on self-consistent calculations, denoted by P1 in the following.

In this paper, we aim at applying the new pairing interaction P1 to describe finite nuclei and to see whether one can provide a universal description of pairing correlations in nuclear matter and finite nuclei. For comparison, we also study three other pairing interactions. We label the pairing interaction of Ref. [11] as P2, which is obtained in the same way as P1 but fitted to pairing gaps of free spectrum instead of the mean field. We also consider a second isovector pairing interaction, referred to as P3, which is extracted from fitting to the experimental OEM using the empirical three-point formula [6]. In addition to the above two isovector types of pairing interactions, we also study an isoscalar pairing interaction, denoted as P4, to check the impact of isospin dependence.

For the mean field part, we use the EV8 code [18,19] with the SkP, SLy4, and SkI4 forces. The particle-particle channel is described by the BCS approximation with the four different pairing interactions detailed above. Experimental binding energies are taken from AME2016 [20].

The paper is organized as follows. In Sec. II, we give a brief introduction of the Skyrme Hartree-Fock plus BCS method (SHF+BCS) and describe the isospin-density-dependent and isoscalar pairing interactions. Numerical details are also presented in this section. Then, we take Ca, Ni, Zr, and Sn isotopes as examples to compare the results of the four effective pairing interactions for the SkP force in Sec. III. Moreover, we adopt the SLy4 and SkI4 forces to study the impacts from the mean field. Finally, we make a brief summary in Sec. IV.

II. THEORETICAL FRAMEWORK

In this section, we briefly review the SHF+BCS method, describe the isospin-density-dependent pairing interactions, and spell out some numerical details.

A. Skyrme force

The Skyrme force is widely used in Hartree-Fock calculations. Its energy density functional contains the same terms as that in Ref. [21]. We adopt the SkP force [22] in our present study, which is obtained by paying particular attention to pairing properties and accurate description of binding energies. The SLy4 force [21], and SkI4 force [23] are also used for comparison.

B. Isospin-density-dependent pairing interactions

As a linear interpolation of the particle-particle interaction between symmetric nuclear matter and pure neutron matter, isospin-density-dependent zero-range effective interactions are derived in Refs. [11,16], for neutrons and protons,

respectively,

$$
\begin{aligned}
g_{\mathrm{n}}(\rho, \beta) &= 1 - \eta_s(\rho/\rho_0)^{\alpha_s}(1-\beta) - \eta_n(\rho/\rho_0)^{\alpha_n}\beta, \\
g_{\mathrm{p}}(\rho, \beta) &= 1 - \eta_s(\rho/\rho_0)^{\alpha_s}(1+\beta) + \eta_n(\rho/\rho_0)^{\alpha_n}\beta,
\end{aligned}
\tag{1}
$$

where the four parameters η_s, η_n, α_s, and α_n are adjusted to reproduce the values of the pairing gaps in infinite nuclear matter. The saturation density ρ_0 of the SNM is $\rho_0 = 0.16$ fm^{-3} and asymmetric parameter $\beta = (\rho_{\mathrm{n}} - \rho_{\mathrm{p}})/(\rho_{\mathrm{n}} + \rho_{\mathrm{p}})$, in which N (Z) is the neutron (proton) number, $A = N + Z$ is mass number and ρ_{n} (ρ_{p}) refers to neutron (proton) density.

The isoscalar pairing interaction reads

$$
g(\rho, \beta = 0) = 1 - \eta_s(\rho/\rho_0)^{\alpha_s},
\tag{2}
$$

where $\eta_s = 1$ and $\alpha_s = 1$.

In the BCS approximation [24], the pairing matrix element reads

$$
\bar{v}^{\mathrm{pair}}_{q,k\bar{k}m\bar{m}} = -V_q \int d^3 r \, g_q(\rho, \beta)\Psi^{\dagger}_k(\boldsymbol{r})\Psi^{\dagger}_{\bar{k}}(\boldsymbol{r})\Psi_m(\boldsymbol{r})\Psi_{\bar{m}}(\boldsymbol{r}),
\tag{3}
$$

where q stands for n or p, $V_q = V_0$ is the pairing strength determined by the scattering length, which reproduces the phase shift in the low energy region for a given cutoff energy, $g(\rho, \beta)$ from Eq. (1) or (2) is the form factor of the isovector or isoscalar pairing interaction, and $\Psi_k(\boldsymbol{r})$ is the wave function of the kth HF single-particle (s.p.) level [25].

C. Pairing energy, binding energy, and pairing gap in the SHF+BCS method

In the SHF+BCS method, the binding energy B of a nucleus can be written as a sum of five parts [19]:

$$
B = -E_{\mathrm{kin}} - E_{\mathrm{Sk}} - E_{\mathrm{Coul}} - E_{\mathrm{pair}} - E_{\mathrm{corr}},
\tag{4}
$$

where E_{kin} is the kinetic energy, E_{Sk} is the Skyrme energy, E_{Coul} is the Coulomb energy, E_{pair} is the pairing energy, and E_{corr} is the center-of-mass correction energy. E_{pair} is the main contribution of the pairing interaction to the binding energy. Other parts of the binding energy, such as E_{Sk}, are functions of the density ρ, and the density ρ is a function of the occupation probability v_k^2 of single-particle levels. Therefore, the binding energy will also be influenced by the pairing interaction through v_k^2.

In particular, the pairing energy E_{pair} can be written in the canonical basis as

$$
E_{\mathrm{pair}} = \sum_{k,m>0} f_k u_k v_k f_m u_m v_m \bar{v}^{\mathrm{pair}}_{k\bar{k}m\bar{m}},
\tag{5}
$$

in which $u_k^2 + v_k^2 = 1$, $\bar{v}^{\mathrm{pair}}_{k\bar{k}m\bar{m}}$ is the pairing matrix element, and

$$
f_k = \left[1 + e^{(\epsilon_k - \lambda_q - E_C)/\mu_q}\right]^{-1/2}\left[1 + e^{(\lambda_q - \epsilon_k - E_C)/\mu_q}\right]^{-1/2}
\tag{6}
$$

is the cutoff factor, where ϵ_k is the energy of the kth s.p. level, λ is the Fermi energy, E_C is the truncation energy of the pairing interaction, and μ_q is fixed to be 0.5 MeV [25]. The set of equations that determine the occupation probability of single-particle states v_k^2 are derived from the variation

TABLE I. Parameters of the pairing interactions studied in the present work, in which P1, P2, and P3 are of isovector type, and P4 is of isoscalar type. E_C is the truncated energy, V_0 is the pairing strength, and η_s, α_s, η_n, and α_n are the parameters of Eq. (1).

Parameters	P1	P2	P3	P4
E_C (MeV)	40	40	5	5
V_0 (MeV fm^3)	542	542	824	1400
η_s	0.729	0.664	0.677	1
α_s	0.522	0.522	0.365	1
η_n	1.010	1.010	0.931	
α_n	0.525	0.525	0.378	

of

$$\frac{\delta}{\delta v_j}\left(2\sum_{k>0}\epsilon_k v_k^2 - \lambda_q\langle \hat{N}_q\rangle + E_{\text{pair}}\right) = 0, \qquad (7)$$

where λ_q is the Lagrange multiplier, which is introduced to obtain the required mean number of protons and neutrons.

The probability of the s.p. state $|k\rangle$ and its time-reversal s.p. state $|\bar{k}\rangle$ being occupied by one pair of neutrons or protons can be expressed as

$$v_k^2 = \left[1 - (\epsilon_k - \lambda_q)\Big/\sqrt{(\epsilon_k - \lambda_q)^2 + f_k^2\Delta_{k\bar{k}}^2}\right]\Big/2, \qquad (8)$$

in which

$$\Delta_{k\bar{k}} = -\sum_{m>0} f_m u_m v_m \bar{v}_{k\bar{k}m\bar{m}}^{\text{pair}} \qquad (9)$$

is the pairing gap of the kth single-particle level.

For odd-A nuclei, we use the blocking method of Ref. [26]. When a pair of s.p states $|k\rangle$ or $|\bar{k}\rangle$ is chosen to be occupied or blocked, the occupied or unoccupied probability in the BCS state is fixed to be $u_k^2 = v_k^2 = 1/2$, and the pairing gap of that s.p. level is fixed to be $\Delta_k = 0$ MeV.

D. Numerical details

The EV8 code solves the HF+BCS equations to obtain binding energies iteratively with the imaginary time step method [27]. For even-even and odd-A nuclei, we use the empirical three-point formula to extract the OEM staggering of isotopes:

$$\Delta_n^{(3)}(N, Z) = -\frac{\pi_N}{2}[B(N+1, Z) - 2B(N, Z) + B(N-1, Z)], \qquad (10)$$

where $B(N, Z)$ is the binding energy of a nucleus, and π_N is the parity of the isotope with neutron number N.

We adopt three isospin-density-dependent pairing interactions, P1 [1], P2 [11,16], and P3 [6], with the isoscalar interaction P4 [6] for comparison, and list the parameters in Table I. One can see that P1 and P2 have the same cutoff energy $E_C = 40$ MeV, which gives the best agreement between the microscopic and contact interactions in the high Fermi momentum region $k_{F_n} > 1$ fm^{-1}. P3 and P4 have a smaller cutoff energy $E_C = 5$ MeV, which is the maximum energy window around the Fermi energy allowed by the old version of EV8 (2005) in Ref. [18]. In our calculations, we use the updated version of EV8 (2015) in Ref. [19], in which the cutoff energy

E_C is taken to be 5 MeV for P3 and P4 and 40 MeV for P1 and P2. As we know, effective pairing interactions are sensitive to the values of the energy (or momentum) cutoff (see, e.g., Fig. 4(a) of Ref. [2] for PNM). Therefore, the parameters are quite different for P2 and P3, especially the potential strength V_0. This will be further analyzed in the following section.

Before large-scale calculations, we check the convergence of OEM staggering with respect to the number of neutron wave functions, i.e., "nwaven" in the EV8 code. It turns out that Δ_n converges within the absolute accuracy 0.03 MeV as $N = 100$. In most calculations, the absolute accuracy of 10^{-4} MeV can be achieved for binding energies. Since the binding energies are at the order of 1000 MeV, the relative accuracy is better than 10^{-7}. However, for some odd-A nuclei, it is difficult to achieve such an accuracy. Therefore, the criterion of convergence is fixed to be 10^{-2} MeV, which corresponds to a relative accuracy 10^{-5}.

III. RESULTS AND DISCUSSIONS

We calculate the binding energies of even-even and odd-A Ca, Ni, Zr, and Sn isotopes with the SkP force, then derive the OEM staggering via the three-point formula of Eq. (10). It is known that pairing gaps obtained from the OEM staggering are not reliable for isotopes with magic or semimagic number $N = 20, 28, 40, 50,$ and 82, such as ^{40}Ca, ^{48}Ca, ^{56}Ni, ^{78}Ni, ^{90}Zr, ^{100}Sn, and ^{132}Sn. Therefore, we ignore the neutron pairing gaps Δ_n for these nuclei in the later analysis.

In Fig. 1, we show the OEM staggering as a function of mass number A for Ca, Ni, Zr, and Sn isotopes with the SkP force. The solid red (dark blue) lines with triangles (squares) refer to the neutron pairing gaps obtained with the isovector pairing interaction P1 (P2), which is extracted from the BHF+BCS calculations for SNM and PNM with the mean field (free) spectrum. The solid green lines with diamonds correspond to the predictions of the isovector pairing interaction P3, which is obtained by fitting to the experimental OEM staggering. While the solid light blue lines with stars denote the results obtained with the isoscalar pairing interaction P4. The black solid circles with error bars labeled by Exp. represent the experimental data. Generally speaking, the neutron pairing gaps $\Delta_n^{(3)}$ obtained with the isovector pairing interactions P1, P2, and P3 are much closer to the experimental data than those from the isoscalar pairing interaction P4. Therefore, the isospin dependence of the pairing interaction seems to be crucial to reproduce the experimental OEM staggering.

To quantitatively evaluate the deviations of the theoretical predictions from the experimental OEM staggering, we calculate the root mean square error (RMSE) of the neutron pairing gaps for all the isovector pairing interactions, except for magic or semimagic nuclei as mentioned above. The RMSE is defined by

$$\sigma = \sqrt{\frac{\sum_{i=1}^{N}(\Delta_{i,\text{cal}} - \Delta_{i,\text{exp}})^2}{N}}, \qquad i = 1, 2, \ldots, N, \qquad (11)$$

where $\Delta_{i,\text{cal}}$ and $\Delta_{i,\text{exp}}$ are the calculated and the experimental OEM staggering of an isotope labeled by i, and N is the
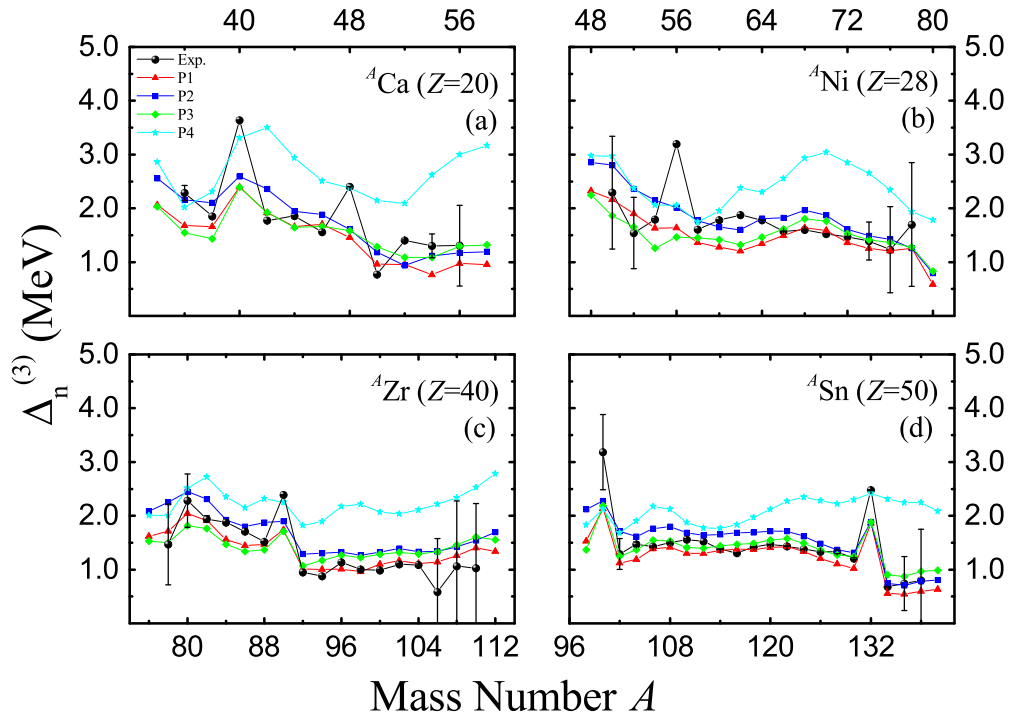
FIG. 1. Odd-even mass staggering as a function of mass number A for Ca, Ni, Zr, and Sn isotopes with the SkP force. P1 (solid red lines with triangles), P2 (solid dark blue lines with squares), and P3 (solid green lines with diamonds) are isovector pairing interactions and P4 (solid light blue lines with stars) is an isoscalar one. The black solid circles with error bars correspond to experimental data.

number of isotopes considered. We list the RMSEs in Table II for a better understanding of the predictions of different pairing interactions in comparison with the experimental data. As mentioned above, the neutron pairing gaps for magic nuclei ^{40}Ca, ^{48}Ca, ^{56}Ni, ^{78}Ni, ^{90}Zr, ^{100}Sn, and ^{132}Sn are omitted in calculating the RMSEs.

For Ni and Zr isotopes, P1 turns out to be the best among the isovector pairing interactions for the SkP force. The RM-SEs of the OEM staggering for Ni, Zr, and Sn isotopes are reduced by 14.3%, 41.0%, and 30.4% respectively, compared with those of P2, which is also extracted from infinite nuclear matter with the BHF method but for free spectrum, instead of the mean field spectrum. Moreover, the predictions of P1 for Ca isotopes are almost the same as those of P2, and are better than those of P3 by ≈5%. One should note that P3 is obtained by fitting to the experimental OEM staggering. In addition,

for Zr isotopes P1 can reduce the RMSEs of OEM staggering by ≈34.3% compared with P3. For Sn isotopes, P1 can also give a better description of OEM staggering than P2 by 30%, but not as good as P3. The results seem to be consistent with the conclusion of Ref. [6] that P3 is particularly good for Sn isotopes together with the SkP force.

To show the predictive power of the pairing interactions, we extend our calculations to neutron-rich nuclei ^{58}Ca, ^{80}Ni, ^{112}Zr, ^{140}Sn, which are plotted in Fig. 1 as well. We have also calculated the OEM scattering of Ca, Ni, Zr, and Sn isotopes with the SLy4 force [21], and found that it does not predict the pairing gaps as well as the SkP force. Generally speaking, it underestimates the pairing gaps compared with measured data and doubles the RMSEs compared to the SkP force for the three isovector pairing interactions. In Table III we list the same RMSEs of the OEM scattering as Table II, but for the SLy4 force. It can be clearly seen that in the SLy4 mean field the OEM scattering results for the P1 interaction are worse than those for the P2 and P3 interactions, mainly because of

TABLE II. RMSE of the OEM staggering of Ca, Ni, Zr, and Sn isotopes in units of MeV and the relative errors for the SkP force. The OEM staggering for magic nuclei ^{40}Ca, ^{48}Ca, ^{56}Ni, ^{78}Ni, ^{90}Zr, ^{100}Sn, and ^{132}Sn are neglected in the calculation of RMSE.

	P1	P2	$\dfrac{\text{P2} - \text{P1}}{\text{P2}}$	P3	$\dfrac{\text{P3} - \text{P1}}{\text{P3}}$	P4	$\dfrac{\text{P4} - \text{P1}}{\text{P4}}$
Ca	0.35	0.33	−6.1%	0.37	5.4%	1.17	70.1%
Ni	0.30	0.35	14.3%	0.30	0.0%	0.94	68.1%
Zr	0.23	0.39	41.0%	0.35	34.3%	1.00	77.0%
Sn	0.16	0.23	30.4%	0.12	−33.3%	0.89	82.0%

TABLE III. Same as Table II, but for the SLy4 force.

	P1	P2	$\dfrac{\text{P2} - \text{P1}}{\text{P2}}$	P3	$\dfrac{\text{P3} - \text{P1}}{\text{P3}}$	P4	$\dfrac{\text{P4} - \text{P1}}{\text{P4}}$
Ca	0.63	0.51	−23.5%	0.60	−5.0%	0.65	3.1%
Ni	0.83	0.70	−18.6%	0.70	−18.6%	0.63	−31.7%
Zr	0.59	0.46	−28.3%	0.47	−25.5%	0.74	20.3%
Sn	0.56	0.35	−60.0%	0.33	−69.7%	0.46	−21.7%

TABLE IV. Same as Table II, but for the SkI4 force.

	P1	P2	$\dfrac{P2-P1}{P2}$	P3	$\dfrac{P3-P1}{P3}$	P4	$\dfrac{P4-P1}{P4}$
Ca	0.78	0.65	-20.0%	0.72	-8.3%	0.70	-11.4%
Ni	0.99	0.89	-11.2%	0.90	-10.0%	0.54	-83.3%
Zr	0.70	0.54	-29.6%	0.58	-20.7%	0.55	-27.3%
Sn	0.72	0.55	-30.9%	0.50	-44.0%	0.37	-94.6%

the underestimation of the pairing gaps in comparison with experimental data. Similar results have been obtained for the SkI4 force [23] and our results are listed in Table IV. These results justify the use of the SkP force in the SHF+BCS model to check the validity of pairing interactions, which confirm the claim of Ref. [22] that the SkP force can give better descriptions of pairing gaps. Note that Skyrme force parameters were not fitted together with the BCS pairing interactions in a global way, so no optimal results should be expected.

IV. SUMMARY

We studied the OEM staggering of Ca, Ni, Zr, and Sn isotopes with the effective pairing interaction P1, together with three other types of pairing interactions for comparison, using the SHF+BCS method with the SkP force. We showed that P1 is suitable for the description of OEM staggering in these isotopes, especially that it is much better than the other pairing interactions for Ni and Zr isotopes. For example, the pairing gaps for Zr isotopes are 41% (34%) better than those obtained with P2 (P3). Our predictions for Ca isotopes are comparable with those of P2 and P3, which is reasonable since the parameters of P3 are obtained by fitting to the experimental OEM staggering [6]. For Sn isotopes, the

predictions of P1 are almost ≈30% better than those of P2, and are comparable with the results of P3. It is quite interesting to find that, although the isospin-density-dependent pairing interaction P1 is extracted from the bare interaction for nuclear matter within the framework of the BHF method, it can give reasonable description of the OEM staggering for Ni, Zr, and Sn isotopes (better than the results obtained with P2). The conclusions will be changed if one chooses other mean fields, such as SLy4 or SkI4. With SkP, P1 is preferred over the others. This is understandable because pairing interactions are closely related to mean fields. Comparing the results shown in Tables III and IV, it is clear that the SkP force together with the BCS treatment of pairing correlations can yield an optimal description of the quantities studied in the present work.

It is interesting to see that, without any tunable parameters, P1 can give pretty good description of the OEM staggering for the SkP force compared with measured data. For some isotopes, e.g., Ca and Zr isotopes (or Ni isotopes), the predictions are even better (or comparable) than those of P3, extracted by fitting to the experimental pairing gaps. From this point of view, it is reasonable to say that neutron pairing gaps of infinite nuclear matter can be a good constraint of the neutron pairing interaction in finite nuclei. In the future, our ansatz could also be tested for proton pairing gaps.

[1] S. S. Zhang, U. Lombardo, and E. G. Zhao, Sci. Chin. Phys. Mech. Astron. **54**, 236 (2011).

[2] S. S. Zhang, L. G. Cao, U. Lombardo, E. G. Zhao, and S. G. Zhou, Phys. Rev. C **81**, 044313 (2010).

[3] D. J. Dean and M. Hjorth-Jensen, Rev. Mod. Phys. **75**, 607 (2003).

[4] J. M. Dong, U. Lombardo, H. F. Zhang, and W. Zuo, Astrophys. J. **817**, 6 (2016).

[5] S. S. Zhang, J. P. Peng, M. S. Smith, G. Arbanas, and R. L. Kozub, Phys. Rev. C **91**, 045802 (2015).

[6] C. A. Bertulani, H. F. Lu, and H. Sagawa, Phys. Rev. C **80**, 027303 (2009).

[7] S. Goriely, N. Chamel, and J. M. Pearson, Phys. Rev. Lett. **102**, 152503 (2009).

[8] N. Hinohara and W. Nazarewicz, Phys. Rev. Lett. **116**, 152502 (2016).

[9] Y. Tian, Z. Y. Ma, and P. Ring, Phys. Lett. B **676**, 44 (2009).

[10] Y. T. Rong, P. W. Zhao, and S. G. Zhou, Phys. Lett. B **807**, 135533 (2020).

[11] J. Margueron, H. Sagawa, and K. Hagino, Phys. Rev. C **77**, 054309 (2008).

[12] N. Chamel, S. Goriely, and J. Pearson, Nucl. Phys. A **812**, 72 (2008).

[13] N. Chamel, Phys. Rev. C **82**, 014313 (2010).

[14] S. Goriely, N. Chamel, and J. M. Pearson, Phys. Rev. C **93**, 034337 (2016).

[15] S. S. Zhang, L. G. Cao, U. Lombardo, and P. Schuck, Phys. Rev. C **93**, 044329 (2016).

[16] J. Margueron, H. Sagawa, and K. Hagino, Phys. Rev. C **76**, 064316 (2007).

[17] L. G. Cao, U. Lombardo, and P. Schuck, Phys. Rev. C **74**, 064301 (2006).

[18] P. Bonche, H. Flocard, and P. Heenen, Comput. Phys. Commun. **171**, 49 (2005).

[19] W. Ryssens, V. Hellemans, M. Bender *et al.*, Comput. Phys. Commun. **187**, 175 (2015).

[20] M. Wang, G. Audi, F. G. Kondev *et al.*, Chin. Phys. C **41**, 030003 (2017).

[21] E. Chabanat, P. Bonche, P. Haensel, J. Meyer, and R. Schaeffer, Nucl. Phys. A **635**, 231 (1998); **643**, 441 (1998).

[22] J. Dobaczewski, H. Flocard, and J. Treiner, Nucl. Phys. A **422**, 103 (1984).

[23] P.-G. Reinhard and H. Flocard, Nucl. Phys. A **584**, 467 (1995).

[24] U. Lombardo and H.-J. Schulze, in *Physics of Neutron Star Interiors*, edited by D. Blaschke, N. K. Glendenning and A. Sedrakian, Lecture Notes in Physics Vol. 578 (Springer-Verlag, Berlin, 2001).

[25] S. Krieger, P. Bonche, H. Flocard *et al.*, Nucl. Phys. A **517**, 275 (1990).

[26] M. Bender, K. Rutz, P.-G. Reinhard, and J. A. Maruhn, Eur. Phys. J. A **8**, 59 (2000).

[27] K. T. R. Davies, H. Flocard, S. Kireger, and M. S. Weiss, Nucl. Phys. A **342**, 111 (1980).